JOC Article
pubs.acs.org/joc

Structure and Dynamics of α-Aryl Amide and Ketone Enolates: THF, PMDTA, TMTAN, HMPA, and Crypt-Solvated Lithium Enolates, and Comparison with Phosphazenium Analogues

Kristopher J. Kolonko, Ilia A. Guzei, and Hans J. Reich*

Department of Chemistry, University of Wisconsin, Madison, Wisconsin 53706

reich@chem.wisc.edu

Received May 21, 2010

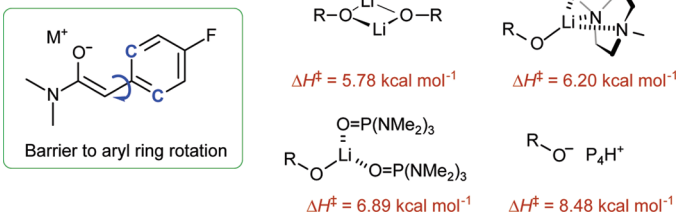

A variety of multinuclear NMR techniques, in combination with X-ray diffraction methods, were used to probe the solution structure of α-aryl lithium enolates of bis(4-fluorobenzyl) ketone (**1-H**), phenyl 4-fluorobenzyl ketone (**2-H**), and *N*,*N*-dimethyl 4-fluorophenylacetamide (**3-H**) in ethereal solvents and in the presence of cosolvent additives PMDTA, TMTAN, HMPA, and cryptand [2.1.1]. All three enolates were dimers in THF solution, and were converted to monomers by the triamine additives, PMDTA and TMTAN. The exchange of the triamine-solvated monomers with their ethereal-solvated dimer counterparts was probed by using dynamic NMR (DNMR). The cosolvent HMPA formed monomers along with minor amounts of lithiate species, $(RO)_2Li^-$ and $(RO)_3Li^{2-}$, which were also observed when cryptand [2.1.1] was used as a cosolvent, or when mixed lithium−phosphazenium enolate solutions were prepared. Dynamic exchange of lithiate species was investigated by DNMR spectroscopy. The barrier to rotation of the conjugated 4-fluorophenyl ring of these diverse enolate structures was measured and found to be consistent with a resonance picture where lower aggregation states lead to increased delocalization of negative charge. The lithium enolate aggregates identified were compared to the "naked" α-4-fluorophenyl enolates generated with the phosphazene base **P4**. The barrier to aryl ring rotation was 2.7 kcal/mol higher for the phosphazenium enolate **3-Li·P4H** compared to the dimer **(3-Li)**$_2$. Structural characterization of a phosphazenium enolate through X-ray crystallography was obtained for the first time. Additional aspects of the Schwesinger base **P4** were investigated which included characterization of the solution exchange behavior of the protonated and unprotonated forms as well as determination of the solid state structure by X-ray diffraction.

Introduction

Lithium enolates are versatile carbon nucleophiles used to introduce substituents α to the carbonyl group in ketones, esters, aldehydes, and amides. Like most lithium species, the aggregation state of enolates has crucial relevance to reactivity and probably selectivity. However, unlike typical organolithium reagents, where information about the aggregation state can often be found from detection of $^{6/7}$Li coupling to carbon, the lithium in enolates is bonded to oxygen, whose poor NMR properties do not provide any insights. Other experimental techniques and measurements have been employed to elucidate lithium enolate solution structures, such as X-ray crystallography,[1,2] colligative property measurements (freezing point depressions and vapor pressure osmometry),[3,4] and singular value decomposition of UV−vis spectra.[5]

(1) Amstutz, R.; Schweizer, W. B.; Seebach, D.; Dunitz, J. D. *Helv. Chim. Acta* **1981**, *64*, 2617–2621. Seebach, D.; Amstutz, R.; Laube, T.; Schweizer, W. B.; Dunitz, J. D. *J. Am. Chem. Soc.* **1985**, *107*, 5403–5409. Seebach, D. *Angew. Chem., Int. Edit. Engl.* **1988**, *27*, 1624–1654. Hahn, E.; Maetzke, T.; Plattner, D. A.; Seebach, D. *Chem. Ber.* **1990**, *123*, 2059–2064.

DOI: 10.1021/jo100970r Published on Web 08/25/2010

Early enolate NMR studies often compared the proton and carbon NMR chemical shifts of lithium, sodium, and potassium enolates in various solvents to gain insight into observed reactivity changes and the associated aggregation states.[6,7a] In general, changing the metal from Li to Na to K and/or increasing the polarity of the solvent causes an increase in the magnitude of the chemical shift differences observed between the enolates and the corresponding enol acetates or enol silyl ethers. Similar comparisons have since been made which have included enolates generated with noncoordinating counterions such as tris(diethylamino)sulfonium[8] and the nonmetallic base P4-*t*Bu (**P4**).[9,10a,b] Unfortunately, these comparisons do not provide any direct information on the aggregation state of the lithium enolates themselves.

Several NMR-based techniques have been developed for the characterization of lithium enolate solution aggregation states. Jackman employed ^{7}Li quadrupole-splitting constants and ^{13}C spin−lattice relaxation times along with ^{13}C NMR chemical shifts of the enolate carbons to estimate the aggregation state as well as the degree of solvation of several lithium enolates.[7a,b,c] This approach was then successfully applied to determine the solution structure of a variety of lithium phenoxides (phenolates),[7c,d] but few others have adopted these methods to study lithium enolates.[11] More recently, Collum and co-workers have utilized NMR spectroscopic determinations of numerous lithium enolate and phenolate solution structures using the method of continuous variance[12a] or the method of Job,[13] a technique in which the symmetry of the homoaggregates is broken by the formation of mixed aggregates.

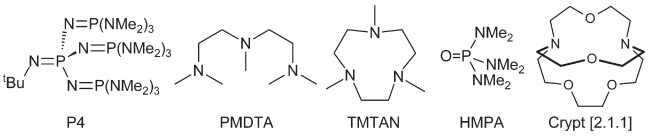

We have explored the utility of titrations of lithium species with hexamethyl phosphoric triamide, HMPA, using NMR spectroscopy as a general tool for determining the aggregation state of organolithium species,[10c−i] and specifically lithium enolates.[10b] Tetrameric enolates (those of cyclopentanone, cyclohexanone, and acetophenone) in THF/Et_2O underwent serial solvation as the concentration of HMPA was increased to the tetra-HMPA solvate (one HMPA per lithium of the tetramer) without dissociation to lower aggregates. Dimeric enolates (lithium enolates of dibenzyl ketone and phenyl benzyl ketone) in THF/Et_2O underwent serial solvation up to 1 equiv of HMPA as well, but additional HMPA resulted in dissociation to monomers. These dimeric enolates were also deaggregated by the triamine cosolvent additives TMTAN and PMDTA, whereas the tetrameric enolates showed no observable effect. While the use of a cosolvent to probe the structure in the absence of that cosolvent has some uncertainty associated with it, a logical progression

(2) Williard, P. G.; Carpenter, G. B. *J. Am. Chem. Soc.* **1985**, *107*, 3345–3346. Williard, P. G.; Hintze, M. J. *J. Am. Chem. Soc.* **1987**, *109*, 5539–5541. Williard, P. G.; Tata, J. R.; Schlessinger, R. H.; Adams, A. D.; Iwanowicz, E. J. *J. Am. Chem. Soc.* **1988**, *110*, 7901–7903. Williard, P. G.; Macewan, G. J. *J. Am. Chem. Soc.* **1989**, *111*, 7671–7672. Williard, P. G.; Hintze, M. J. *J. Am. Chem. Soc.* **1990**, *112*, 8602–8604. Henderson, K. W.; Dorigo, A. E.; Williard, P. G.; Bernstein, P. R. *Angew. Chem., Int. Ed. Engl.* **1996**, *35*, 1322–1324. Henderson, K. W.; Dorigo, A. E.; Liu, Q.-Y.; Williard, P. G.; Schleyer, P. v. R.; Bernstein, P. R. *J. Am. Chem. Soc.* **1996**, *118*, 1339–1347. Sun, C. Z.; Williard, P. G. *J. Am. Chem. Soc.* **2000**, *122*, 7829–7830.

(3) Arnett, E. M.; Palmer, C. A. *J. Am. Chem. Soc.* **1990**, *112*, 7354–7360. Arnett, E. M.; Fisher, F. J.; Nichols, M. A.; Ribeiro, A. A. *J. Am. Chem. Soc.* **1990**, *112*, 801–808. Arnett, E. M.; Moe, K. D. *J. Am. Chem. Soc.* **1991**, *113*, 7288–7293.

(4) Shobatake, K.; Nakamoto, K. *Inorg. Chim. Acta* **1970**, *4*, 485–487. Halaska, V.; Lochmann, L. *Collect. Czech. Chem. Commun.* **1973**, *38*, 1780–1782. Denbesten, R.; Harder, S.; Brandsma, L. *J. Organomet. Chem.* **1990**, *385*, 153–159.

(5) (a) Abbotto, A.; Streitwieser, A. *J. Am. Chem. Soc.* **1995**, *117*, 6358–6359. Abu-Hasanayn, F.; Streitwieser, A. *J. Am. Chem. Soc.* **1996**, *118*, 8136–8137. Streitwieser, A.; Wang, D. Z.; Stratakis, M.; Facchetti, A.; Gareyev, R.; Abbotto, A.; Krom, J. A.; Kilway, K. V. *Can. J. Chem.* **1998**, *76*, 765–769. Leung, S. S. W.; Streitwieser, A. *J. Am. Chem. Soc.* **1998**, *120*, 10557–10558. Streitwieser, A.; Wang, D. Z. R. *J. Am. Chem. Soc.* **1999**, *121*, 6213–6219. Leung, S. S. W.; Streitwieser, A. *J. Org. Chem.* **1999**, *64*, 3390–3391. Streitwieser, A.; Juaristi, E.; Kim, Y.-J.; Pugh, J. K. *Org. Lett.* **2000**, *2*, 3739–3741. Wang, D. Z.; Streitwieser, A. *J. Org. Chem.* **2003**, *68*, 8936–8942. (b) Facchetti, A.; Streitwieser, A. *J. Org. Chem.* **1999**, *64*, 2281–2286. Krom, J. A; Streitwieser, A. *J. Org. Chem.* **1996**, *61*, 6354–6359. (c) Gareyev, R.; Ciula, J. C.; Streitwieser, A. *J. Org. Chem.* **1996**, *61*, 4589–4593.

(6) (a) Stork, G.; Hudrlik, P. F. *J. Am. Chem. Soc.* **1968**, *90*, 4464–4465. (b) House, H. O.; Prabhu, A. V.; Phillips, W. V. *J. Org. Chem.* **1976**, *41*, 1209–1214.

(7) (a) Jackman, L. M.; Haddon, R. C. *J. Am. Chem. Soc.* **1973**, *95*, 3687–3692. (b) Jackman, L. M.; Szeverenyi, N. M. *J. Am. Chem. Soc.* **1977**, *99*, 4954–4962. Jackman, L. M.; Scarmoutzos, L. M.; Debrosse, C. W. *J. Am. Chem. Soc.* **1987**, *109*, 5355–5361. (c) Jackman, L. M.; Bortiatynski, J. *Advances in Carbanion Chemistry* **1992**, *1*, 45–87. (d) Jackman, L. M.; Debrosse, C. W. *J. Am. Chem. Soc.* **1983**, *105*, 4177–4184. Jackman, L. M.; Smith, B. D. *J. Am. Chem. Soc.* **1988**, *110*, 3829–3835. Jackman, L. M.; Rakiewicz, E. F.; Benesi, A. J. *J. Am. Chem. Soc.* **1991**, *113*, 4101–4109. Jackman, L. M.; Chen, X. *J. Am. Chem. Soc.* **1992**, *114*, 403–411. Jackman, L. M.; Cizmeciyan, D. *Magn. Reson. Chem.* **1996**, *34*, 14–17. Jackman, L. M.; Chen, X. *J. Am. Chem. Soc.* **1997**, *119*, 8681–8684. (e) Jackman, L. M.; Lange, B. C. *J. Am. Chem. Soc.* **1981**, *103*, 4494–4499.

(8) Noyori, R.; Nishida, I.; Sakata, J. *J. Am. Chem. Soc.* **1983**, *105*, 1598–1608.

(9) Solladie-Cavallo, A.; Liptaj, T.; Schmitt, M.; Solgadi, A. *Tetrahedron Lett.* **2002**, *43*, 415–418. Solladie-Cavallo, A.; Roche, D.; Fischer, J.; DeCian, A. *J. Org. Chem.* **1996**, *61*, 2690–2694.

(10) (a) Kolonko, K. J.; Reich, H. J. *J. Am. Chem. Soc.* **2008**, *130*, 9668–9669. (b) Kolonko, K. J.; Biddle, M. M.; Guzei, I. A.; Reich, H. J. *J. Am. Chem. Soc.* **2009**, *131*, 11525–11534. (c) Reich, H. J.; Green, D. P. *J. Am. Chem. Soc.* **1989**, *111*, 8729–8731. Reich, H. J.; Dykstra, R. R. *Angew. Chem., Int. Ed. Engl.* **1993**, *32*, 1469–1470. Reich, H. J.; Borst, J. P.; Dykstra, R. R. *Organometallics* **1994**, *13*, 1–3. Reich, H. J.; Dykstra, R. R. *Organometallics* **1994**, *13*, 4578–4585. Reich, H. J.; Kulicke, K. J. *J. Am. Chem. Soc.* **1996**, *118*, 273–274. (d) Reich, H. J.; Green, D. P.; Medina, M. A.; Goldenberg, W. S.; Gudmundsson, B. Ö.; Dykstra, R. R.; Phillips, N. H. *J. Am. Chem. Soc.* **1998**, *120*, 7201–7210. (e) Reich, H. J.; Goldenberg, W. S.; Sanders, A. W.; Jantzi, K. L.; Tzschucke, C. C. *J. Am. Chem. Soc.* **2003**, *125*, 3509–3521. (f) Jantzi, K. L.; Puckett, C. L.; Guzei, I. L.; Reich, H. J. *J. Org. Chem.* **2005**, *70*, 7520–7529. (g) Jantzi, K. L.; Guzei, I. L.; Reich, H. J. *Organometallics* **2006**, *25*, 5390–5395. (h) Reich, H. J.; Borst, J. P.; Dykstra, R. R. *Tetrahedron* **1994**, *50*, 5869–5880. (i) Reich, H. J.; Borst, J. P.; Dykstra, R. R.; Green, D. P. *J. Am. Chem. Soc.* **1993**, *115*, 8728–8741. (j) Triple ions of aryllithium reagents were also dentified by mixing experiements: Reich, H. J.; Sikorski, W. H.; Gudmundsson, B. Ö.; Dykstra, R. R. *J. Am. Chem. Soc.* **1998**, *120*, 4035–4036. (k) Reich, H. J.; Goldenberg, W. S.; Gudmundsson, B. O.; Sanders, A. W.; Kulicke, K. J.; Simon, K.; Guzei, I. A. *J. Am. Chem. Soc.* **2001**, *123*, 8067–8079. (l) Jones, A. C.; Sanders, A. W.; Bevan, M. J.; Reich, H. J. *J. Am. Chem. Soc.* **2007**, *129*, 3492–3493. (m) Sikorski, W. H.; Sanders, A. W.; Reich, H. J. *Magn. Reson. Chem.* **1998**, *36*, S118–S124. Reich, H. J.; Sikorski, W. H.; Sanders, A. W.; Jones, A. C.; Plessel, K. N. *J. Org. Chem.* **2009**, *74*, 719–729.

(11) Wen, J. Q.; Grutzner, J. B. *J. Org. Chem.* **1986**, *51*, 4220–4224.

(12) (a) Gruver, J. M.; Liou, L. R.; McNeil, A. J.; Ramirez, A.; Collum, D. B. *J. Org. Chem.* **2008**, *73*, 7743–7747. Liou, L. R.; McNeil, A. J.; Ramirez, A.; Toombes, G. E. S.; Gruver, J. M.; Collum, D. B. *J. Am. Chem. Soc.* **2008**, *130*, 4859–4868. Liou, L. R.; McNeil, A. J.; Toombes, G. E. S.; Collum, D. B. *J. Am. Chem. Soc.* **2008**, *130*, 17334–17341. De Vries, T. S.; Goswami, A.; Liou, L. R.; Gruver, J. M.; Jayne, E.; Collum, D. B. *J. Am. Chem. Soc.* **2009**, *131*, 13142–13154. (b) Kim, Y- J.; Bernstein, M. P.; Roth, A. S. G.; Romesberg, F. E.; Williard, P. G.; Fuller, D. J.; Harrison, A. T.; Collum, D. B. *J. Org. Chem.* **1991**, *56*, 4435–4439. Romesberg, F. E.; Collum, D. B. *J. Am. Chem. Soc.* **1994**, *116*, 9198–9202. (c) McNeil, A. J.; Collum, D. B. *J. Am. Chem. Soc.* **2005**, *127*, 5655–5661. (d) Lucht, B. L.; Bernstein, M. P.; Remenar, J. F.; Collum, D. B. *J. Am. Chem. Soc.* **1996**, *118*, 10707–10718. (e) Lucht, B. L.; Collum, D. B. *J. Am. Chem. Soc.* **1996**, *118*, 2217–2225. (f) Galiano-Roth, A. S.; Collum, D. B. *J. Am. Chem. Soc.* **1988**, *110*, 3546–3553.

(13) Job, P. *Ann. Chim. Appl.* **1928**, *9*, 113–203.

of NMR signals usually provides a clear indication of aggregate structures using these methods.

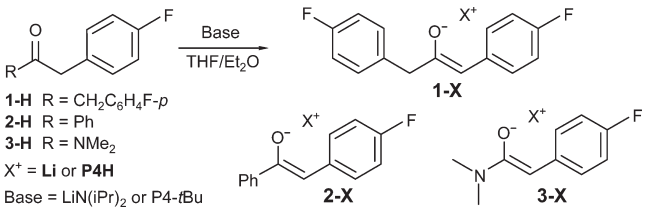

In addition to the standard lithium aggregates (cubic tetramers, 4-centered dimers, contact ion pair monomers), several other more complex ionic species were identified during the course of our enolate studies. Lithium ate complexes of the type $(RO)_2Li^-$ and $(RO)_3Li^{2-}$ were identified under lithium cation deficient conditions for the enolate of 1,3-bis(4-fluorophenyl)-2-propanone (**1-H**). Because of the diversity of structures identified for **1-H** we extended the investigated to the related enolate of ketone **2-H**, as well as amide **3-H**, since there is less information on amide enolate solution structures.[5b,12b,c,14a,15a]

Results and Discussion

Ketone Lithium Enolate Dimers. Previously we have communicated the solution structure of **2-Li** and **1-Li** generated with lithium diisopropylamide (LDA).[10b] Both were found to be primarily dimeric in THF/Et_2O solutions, consistent with earlier findings.[5c] Kinetic enolization of **1-H** with LDA was found to produce a 72:28 mixture of *E* and *Z* enolate isomers, whereas enolization of **2-H** with LDA produced a 22:78 *E* and *Z* enolate mixture based on analysis of the $(CH_3)_3SiCl$ quenched products.[16] Thermal equilibration of both enolates produced predominately (>95%) *Z* enolate, solutions of which were stable under inert atmosphere at room temperature for months. The thermodynamically stable *Z* isomer was used exclusively in the experiments described below. Comparison of *Z*-**2-Li** and *Z*-**1-Li** to their trimethylsilyl counterparts (Table 1) shows that the ^{13}C NMR signal of the β-vinyl carbon of the enolate shifted upfield by about 14 ppm, those of the monomers (vide infra) by ca. 17 ppm, and the "naked" phosphazenium enolates >20 ppm. Similarly, the ^{19}F NMR signal[17] of the dimers was shifted upfield by 6 ppm, compared to 9 ppm for monomers and 12 ppm for the phosphazenium enolates.

Storage of THF/Et_2O solutions of **2-Li** at −78 °C produced crystals which were suitable for X-ray diffraction analysis. There are two dimeric lithium complexes in the unit cell.

TABLE 1. Key Enolate ^{13}C and ^{19}F NMR Chemical Shifts

compound	O—C═C	$\Delta\delta^a$	$\delta^{19}F$	$\Delta\delta^a$
2-SiMe$_3$	109.5	0	−116.3	0
1-SiMe$_3$	109.4	0	−117.6	0
3-SiMe$_3$	88.8	0	−122.6	0
(2-Li)$_2$	95.3	14.2	−123.2	6.9
(1-Li)$_2$	96.1	13.3	−123.9	6.3
(3-Li)$_2$	74.3	14.5	−128.6	6.0
2-Li·TMTAN	92.1	17.4	−124.8	8.5
1-Li·TMTAN	93.5	15.9	−125.9	8.3
3-Li·TMTAN	71.4	17.4	−131.1	8.5
2-Li·PMDTA	91.6	17.9	−125.4	9.1
1-Li·PMDTA	91.8	17.6	−126.4	8.8
3-Li·PMDTA	70.8	18.0	−131.5	8.9
2-Li·$HMPA_2$	90.1	19.4	−127.3	11.0
1-Li·$HMPA_2$	89.6	19.8	−127.7	10.1
3-Li·$HMPA_2$	70.3	18.5	−134.7	12.1
2-TI (P4H)	90.6	18.9	−126.5	10.2
1-TI (P4H)	89.7	19.7	−128.0	10.4
3-TI (P4H)	70.5	18.3	−133.0	10.4
2-P4H	87.1	22.4	−128.9	12.6
1-P4H	87.3	22.1	−130.2	12.6
3-P4H	68.6	20.2	−135.6	13.0

[a]The difference in chemical shift between the enolate and the enol silyl ether.

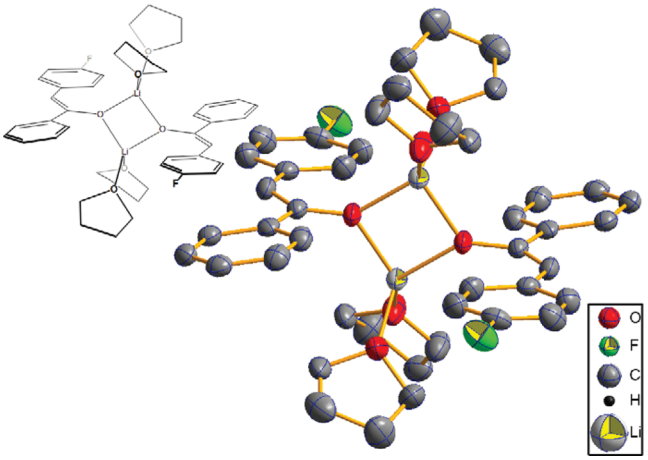

FIGURE 1. Molecular drawing with 50% probability ellipsoids of **(2-Li)$_2$**·$(THF)_4$ determined by single crystal X-ray analysis. All hydrogens, minor components of the disordered atoms, and the noncoordinated THF molecules are omitted for clarity.

Each one resides on a crystallographic inversion center with only one-half of each complex being symmetry independent. Thus, the asymmetric unit contained two halves of the complex, i.e. one-half from each lithium enolate dimer. Each lithium enolate dimer is coordinated to four THF molecules, and two additional THF molecules not coordinated to the lithiums were present in the asymmetric unit. Consequently, the crystal was formed by [**(2-Li)**$THF_2]_2$·2THF (Figure 1).

Amide Lithium Enolate Dimers. Enolization of *N*,*N*-dimethyl 4-fluorophenylacetamide (**3-H**) with LDA in THF/Et_2O produced a single set of signals for the enolate **3-Li** in the ^7Li, ^{13}C, and ^{19}F NMR spectra. Thermal equilibration did not produce observable change in the NMR spectra indicating that the kinetic and thermodynamic enolates were identical. Trimethylsilyl chloride quench products did not survive normal workup procedures for enol silyl ethers, but the enol silyl ether **3-TMS** was sufficiently stable in THF/Et_2O to allow direct NMR analysis of the quenched solution.

(14) (a) Bordwell, F. G.; Fried, H. E. *J. Org. Chem.* **1981**, *46*, 4327–4331. (b) Bordwell, F. G.; Harrelson, J. A., Jr. *Can. J. Chem.* **1990**, *68*, 1714–1718. (c) Bordwell, F. G.; Cornforth, F. J. *J. Org. Chem.* **1978**, *43*, 1767–1768.

(15) (a) Kim, Y.-J.; Streitwieser, A.; Chow, A.; Fraenkel, G. *Org. Lett.* **1999**, *1*, 2069–2071. (b) Fraenkel, G.; Chen, X.; Gallucci, J.; Ren, Y. *J. Am. Chem. Soc.* **2008**, *130*, 4140–4145. Fraenkel, G.; Geckle, J. M. *J. Am. Chem. Soc.* **1980**, *102*, 2869. Fraenkel, G.; Martin, K. V. *J. Am. Chem. Soc.* **1995**, *117*, 10336–10344. (c) Fraenkel, G.; Chow, A.; Winchester, W. R. *J. Am. Chem. Soc.* **1990**, *112*, 6190–6198.

(16) See the Supporting Information for additional experiments and more details.

(17) We have used fluorine-substituted enolates to take advantage of the excellent properties of ^{19}F NMR spectroscopy to analyze enolate solutions. Previous investigations have examined and compared the behavior of several 4-fluoro-substituted and nonsubstituted ketone enolates[10a,b] and have found that the addition of a 4-fluoro substituent did not significantly perturb their properties (for example, the pK_a of acetophenone and 4-fluoroacetophenone in DMSO are 24.7 and 24.5, respectively[14c]).

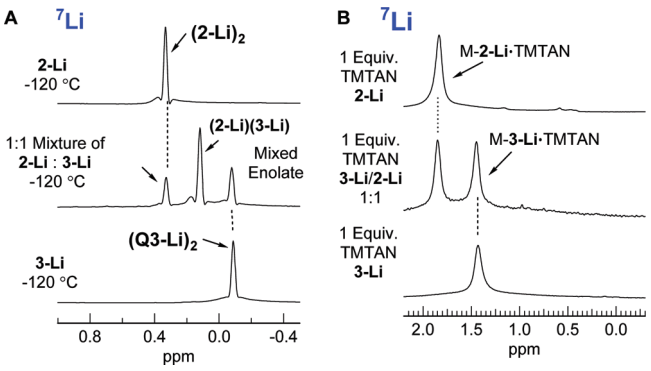

FIGURE 2. ^{7}Li NMR spectra of mixing experiments of **2-Li** and **3-Li** in 3:2 THF/Et_2O at −120 °C. (A) Mixing of the dimeric THF solvates, showing the formation of a mixed dimer. (B) Mixing the monomeric TMTAN complexes formed no new species.

The only isomer formed was of *Z* configuration based on the observed NOE interactions[16] in the ^{1}H-NOESY spectra.

The aggregation state of **3-Li** was established by several mixing experiments with the (*Z*) isomers of **2-Li** and **1-Li**, both known dimeric enolates (Figure 2A[16]).[10b] Mixtures of **3-Li** with either **2-Li** or **1-Li** produced only a single new species in the ^{7}Li, ^{13}C, and ^{19}F NMR spectra. We conclude that despite its substantially higher basicity compared to **2-Li**,[18] the amide enolate **3-Li** was also dimeric in THF/Et_2O solution, and the new species was the mixed dimer. This conclusion was supported by several other experiments described below, and is consistent with the earlier observation by Streitwieser and Cornforth that the lithium enolate of *N*,*N*-dimethyl *p*-biphenylylacetamide is largely dimeric in THF, as determined by the UV/vis SVD technique.[5b]

For the ketones **1-H** or **2-H**, no indication of interactions between the lithium enolates and the neutral carbonyl compounds were detected. Presumably the ketone is insufficiently basic to compete with THF solvation. In contrast, when an excess of amide **3-H** was present with **3-Li**, at < -100 °C new species were observed in slow exchange with the parent lithium enolate dimer.[16] These signals in the ^{13}C and ^{19}F NMR spectra were shifted in the direction of stronger solvation, and were assigned to amide-solvated lithium enolate dimers: [(**3-Li**)$_2$·(**3-H**)$_n$]. Up to 0.5 equiv of **3-H** only the mono- and possibly bis-solvate was detected. We estimate $K_{eq} = 34\ M^{-1}$ for the equilibrium (**3-Li**)$_2$ + **3-H** ⇄ (**3-Li**)$_2$·**3-H**. At higher equivalents new ^{7}Li and ^{19}F NMR signals were detected corresponding to double amide coordination to one lithium, presumably the tris- and tetra-solvates. The formation of such solvates is likely to produce serious complications in kinetic studies of amide enolate reactions.

Triamine-Solvated Lithium Enolate Monomers. The triamine solvent additives PMDTA and TMTAN have been previously shown to convert dimeric **1-Li** to monomers in THF/Et_2O.[10b,19] **2-Li** and **3-Li** showed similar behavior. Upfield shifts of 3−4 ppm were observed for the β-enolate

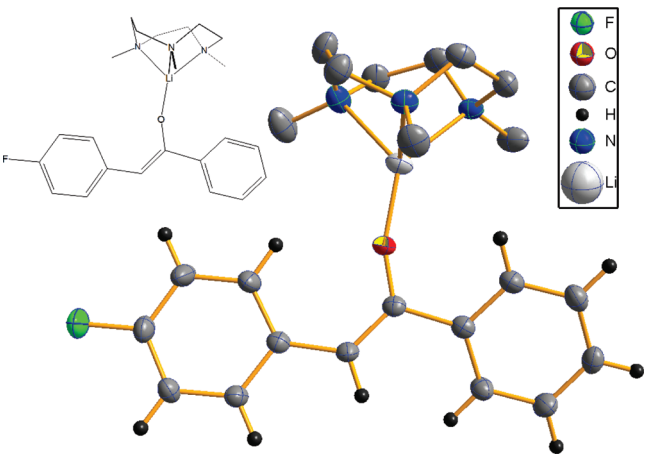

FIGURE 3. Molecular drawing with 50% probability ellipsoids of **2-Li**·TMTAN determined by single crystal X-ray analysis. All minor components of the disordered atoms and hydrogen atoms of the TMTAN ligand are omitted for clarity.

^{13}C NMR signals, and 2−2.5 ppm for the ^{19}F NMR signal (Table 1), consistent with the increased charge polarization of a less aggregated species. In contrast to the THF-solvated dimers (Figure 2A), a mixing experiment of TMTAN-complexed **2-Li** and **3-Li** showed no additional species (Figure 2B), as expected for monomers.

The assignment of a monomeric structure to the triamine bound lithium enolates of **1-Li** was supported by a single-crystal X-ray structure of **1-Li**·PMDTA.[10b] Crystals grown from solutions of **2-Li** and TMTAN showed a monomeric TMTAN complex (Figure 3). Like the other enolates of **2-H** (Figures 1 and 7), this enolate anion was disordered over two positions (roughly related by a 2-fold axis) in a 92:8 ratio.

While both triamine additives tend to produce monomeric enolates, the cyclic variant, TMTAN, is generally more effective at generating monomers than the open chain triamine PMDTA. Free TMTAN cannot be detected until 1 equiv had been added to solutions of the lithium enolates **1-Li**, **2-Li**, and **3-Li**. We estimate that for the equilibrium of eq 1 (R′, R′ = CH_2CH_2), K_{eq} is $>10^5\ M^{-1}$ for all three enolates. In contrast, at 1 equiv of PMDTA, 40% of **1-Li** dimer ($K_{eq} = 32\ M^{-1}$), 55% of **2-Li** dimer ($K_{eq} = 4\ M^{-1}$), and 38% of **3-Li** dimer ($K_{eq} = 57\ M^{-1}$) are present when the enolate concentration is ca. 0.1 M.

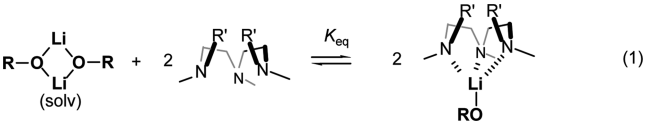

(1)

The rate of exchange of the TMTAN- and PMDTA-solvated enolate monomers with the parent lithium enolate dimers of **2-H** and **3-H** was examined by using multinuclear DNMR techniques. The data were interpreted as a simple two-site exchange, as was done for previous studies of triamine-solvated lithium aggregates.[15c] We will discuss the information for **3-Li** here, but very similar behavior was seen for **2-Li**. The rate of exchange of **3-Li**·TMTAN with the

(18) The pK_a in DMSO of 1,2-diphenylpropanone is 17.7,[14b] that of 1,3-diphenyl-2-propanone is 18.7,[14c] and that of *N*,*N*-dimethylphenylacetamide is 26.6.[14a] The pK_a values of **1-H**, **2-H**, and **Q3-H** would be expected to be within 0.2 units of their *p*-H analogues.[17]

(19) Other dimeric lithium reagents also form monomers with PMDTA and/or TMTAN: phenyllithium,[10d] 3-methoxyphenyllithium,[20] 2-methoxymethylphenyllithium,[10e] thienyllithium,[10f] lithiophenyloxazolines,[10g] neopentyllithium,[15c] lithium bis(trimethylsilyl)amide.[12d]

(20) Eppers, O.; Günther, H. *Helv. Chim. Acta* **1992**, *75*, 2553–2562.

(21) Harder, S.; Boersma, J.; Brandsma, L.; van Mier, G. P. M.; Kanters, J. A. *J. Organomet. Chem.* **1989**, *364*, 1–15.

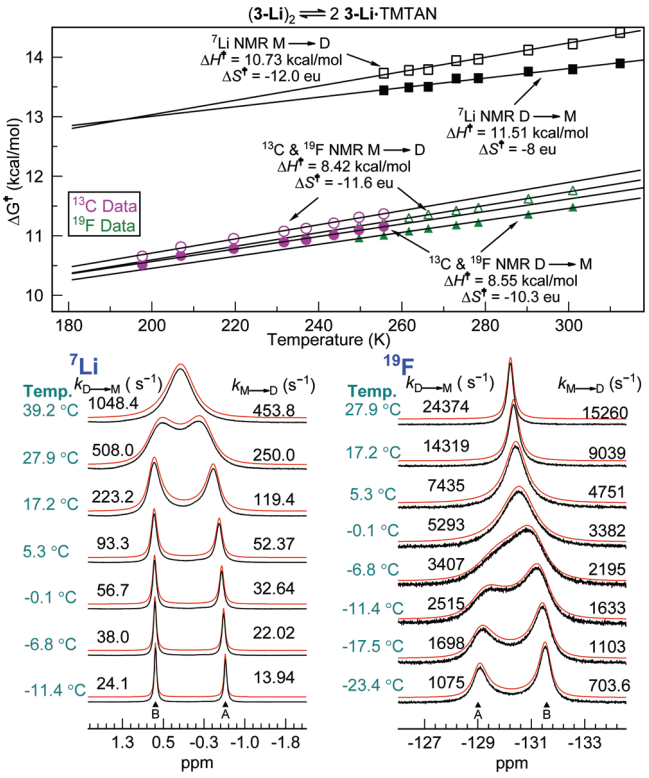

FIGURE 4. DNMR study of the exchange of $(\mathbf{3\text{-}Li})_2$ (signal A) with **3-Li**·TMTAN (signal B) in THF/Et_2O. The red traces are simulations of two-site exchange[24] with the rate constants shown.

dimer derived from line shape analysis of the ^{13}C or ^{19}F NMR signals of the enolate was approximately 50 times as fast as the rate derived from the ^{7}Li NMR signals (Figure 4). This requires a mechanism where the TMTAN ligand remains coordinated to lithium while the dimer and monomer enolate moieties trade places.[22] Although an exact mechanism of exchange is not defined by these experiments, we propose a process like that in eq 2, where uncomplexed monomer in equilibrium with the dimer forms a half-TMTAN-coordinated dimer (**4** with pentacoordinate lithium[23]), which then dissociates, resulting in exchange of enolate (but not lithium) environments.

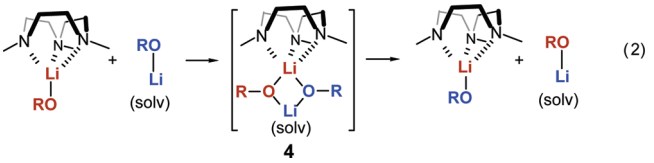

(2)

In contrast, the rates of the dimer and PMDTA-complexed monomer exchange derived from the ^{7}Li, ^{13}C, and ^{19}F NMR signals of **3-Li** were identical. Additionally, free PMDTA exchanged with the Li-complexed PMDTA at comparable rates. The exchange is associative, at least for the ketone, since the rate of conversion of $(\mathbf{2\text{-}Li})_2$ to **2-Li**·PMDTA, measured by injection of PMDTA into a solution of $(\mathbf{2\text{-}Li})_2$ ($t_{1/2} < 2$ s at −125 °C), was at least 80 times as fast as the rate of dissociation of the dimer, as measured by a crossover experiment in which $(\mathbf{1\text{-}Li})_2$ was injected into a solution of $(\mathbf{2\text{-}Li})_2$ to form mixed dimer ($t_{1/2}$ = 165 s at −125 °C). Thus conversion of dimer to PMDTA-complexed monomer occurs by complexation of dimer to PMDTA to form **4**, followed by dissociation. In the PMDTA process **4** dissociates to uncomplexed dimer faster than it dissociates to monomers, whereas for TMTAN dissociation to monomers is faster than loss of ligand. The difference in behavior between TMTAN and PMDTA clearly shows the higher kinetic lithium affinity of TMTAN.

These experiments show that TMTAN is more efficient at promoting monomer formation, and complexes more strongly to lithium than does PMDTA. On the other hand, the NMR chemical shifts of PMDTA complexes of **2-Li**, **1-Li**, and **3-Li**, consistently showed upfield shifts in both the O—C=**C** enolate carbons (from 0.4 to 1.7 ppm) as well as for the ^{19}F NMR signals (0.5 to 0.6 ppm) compared to the TMTAN analogues. Thus the PMDTA complexed enolates have increased charge delocalization (this is also reflected in a higher barrier to phenyl ring rotation discussed below). The higher affinity of TMTAN can be understood in terms of more preorganization of the ligand, and perhaps less steric interaction between ligand and enolate (the average O−Li−N angle is 127.1° in the TMTAN complex, and 119.3° in the PMDTA complex). The higher charge polarization of PMDTA complexes may result from greater flexibility of this ligand, which results in more weakening of the O−Li bond by a more effective interaction between the lithium and nitrogens and more favorable cancellation of ligand and C−Li dipoles.

HMPA-Solvated Lithium Enolate Monomers. The interaction of **1-Li** and **2-Li** with hexamethylphosphoric triamide (HMPA) has been previously reported in detail and used to support the assignment of a dimeric structure to these enolates.[10b] The HMPA titration of **3-Li** (Figure 5) is also consistent only with a dimeric structure. Addition of 0.25 and 0.5 equiv of HMPA produces a new species, the mono-HMPA-solvated dimer (D-h_1), as shown by the doublet and singlet in the ^{7}Li NMR spectrum (one lithium is solvated by HMPA, the other not). The observation of a single set of new signals in the ^{13}C and ^{19}F NMR spectra also requires this structure; higher aggregates must give multiple signals for the first solvate. All signals move in the expected direction of higher charge polarization. At 1 equiv of HMPA, the dominant species is a bis-HMPA dimer (D-h_2) characterized by one set of ^{13}C NMR signals for the enolate carbons, one ^{19}F NMR signal (1.3 ppm upfield from the D-h_1), and one doublet in the ^{7}Li spectrum. Also formed are the mono- and bis-HMPA-solvated enolate monomers (M-h_1 and M-h_2) whose ^{19}F NMR signals are shifted upfield 1.6 and 2.5 ppm from D-h_2, respectively.[25]

(22) A similar effect has been detected for an HMPA-complexed lithiodithiane, which underwent more rapid exchange of the carbanion ligand between two HMPA solvates than exchange of the lithium counterions.[10i]

(23) Pentacoordinate lithiums have been detected for chelated aryllithium species[10e] and lithium amides.[12e]

(24) The DNMR line shape simulations were performed with an updated version of WINDNMR, using a two- or three-site exchange of fluorine triplet of triplets ($^{3}J_{F-H}$ = 8.5 Hz, $^{4}J_{F-H}$ = 5.5 Hz) in the ^{1}H coupled ^{19}F NMR spectra. Reich, H. J. WinDNMR Dynamic NMR Spectra for Windows. *J. Chem. Ed. Software*, Series D, **1996**, *3D*, No. 2 (http://www.chem.wisc.edu/areas/reich/plt/windnmr.htm).

(25) Other dimers (lithium chloride,[10i] phenyllithium,[10d] 2-dimethylaminomethylphenyllithium,[10k] lithiophenylacetonitrile[26]) behave similarly with HMPA.

(26) Carlier, P. R.; Lo, C. W.-S. *J. Am. Chem. Soc.* **2000**, *122*, 12819–12823.

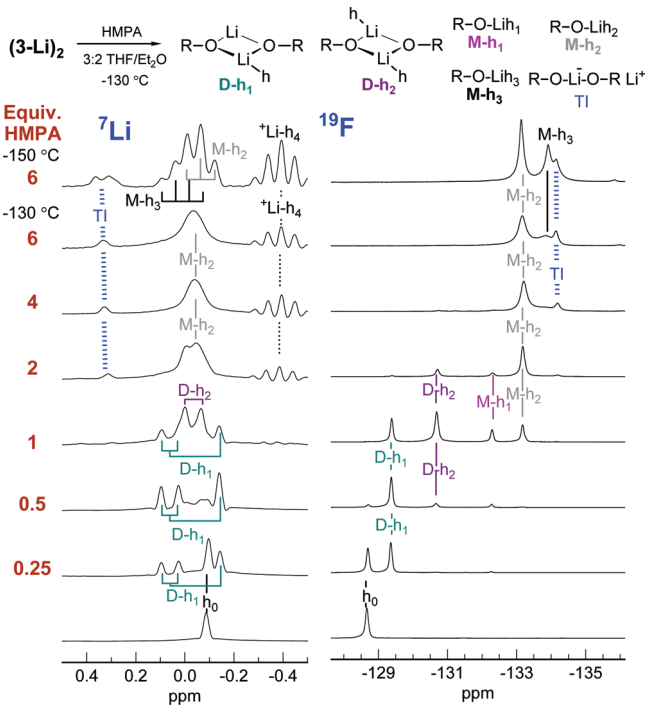

FIGURE 5. HMPA titration of **3-Li** in THF/Et_2O followed by ^7Li and ^{19}F NMR spectroscopy at −130 °C, top spectrum at −150 °C (h = HMPA).

The bis-HMPA-solvated monomer (M-h_2) became the predominant species at the expense of D-h_2 and M-h_1 on the addition of 2 equiv of HMPA. A significant amount of a tetra-HMPA-solvated lithium cation signal ($^+Lih_4$) appears in the ^7Li NMR spectrum (quintet at δ −0.5), associated with a broad, upfield ^7Li singlet (δ 0.3) and a new ^{19}F NMR signal. These signals (which continue to increase as more HMPA was added) can be assigned to a lithium ate complex, the triple ion $(RO)_2Li^-$ (**3-TI**). A second new ^{19}F NMR signal appears downfield from the M-h_2 signal, which has been assigned to tris-HMPA-solvated monomer (M-h_3). Cooling the sample to −150 °C slows the exchange between M-h_2 and M-h_3 and allows the triplet and quartet (due to the $^7Li-^{31}P$ J coupling) to be partially resolved in the ^7Li NMR spectrum. Interestingly, at −150 °C, the singlet at δ 0.3 in the ^7Li NMR spectrum assigned to the internal lithium of the triple ion (**TI**) appears to form a doublet suggesting coordination to HMPA.[16]

The dimeric nature of the **TI** species was confirmed by a mixing experiment where a solution of **3-Li** and **1-Li** was treated with 6 equiv of HMPA.[16] The signals previously assigned to the HMPA-solvated monomers and $^+Li-h_4$ of both enolates show no change. However, one new signal appears at a chemical shift between the **TI** signals of **3-Li** and **1-Li** corresponding to the mixed **TI**, supporting the dimeric stoichiometry.

(27) Schwesinger, R.; Schlemper, H. *Angew. Chem., Int. Ed. Engl.* **1987**, *26*, 1167–1169. Schwesinger, R.; Hasenfratz, C.; Schlemper, H.; Walz, L.; Peters, E. M.; Peters, K.; von Schnering, H. G. *Angew. Chem., Int. Ed. Engl.* **1993**, *32*, 1361–1363. Schwesinger, R.; Schlemper, H.; Hasenfratz, C.; Willaredt, J.; Dambacher, T.; Breuer, T.; Ottaway, C.; Fletschinger, M.; Boele, J.; Fritz, H.; Putzas, D.; Rotter, H. W.; Bordwell, F. G.; Satish, A. V.; Ji, G. Z.; Peters, E. M.; Peters, K.; von Schnering, H. G.; Walz, L. *Liebigs Ann.* **1996**, 1055–1081.

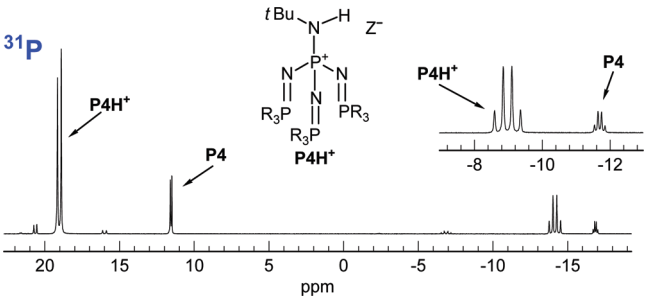

FIGURE 6. ^{31}P NMR spectrum of the protonated (**P4H**$^+$) and unprotonated forms of phosphazene base **P4** in 3:2 THF/Et_2O at −120 °C.

Ketone Phosphazenium Enolates. The strong, metal-free noncoordinating base P4-*t*Bu[27] (**P4**) is well-suited for multinuclear NMR studies. The small number of ^{13}C and ^1H NMR signals minimize overlap with substrate signals, and ^{31}P NMR provides valuable information as to the extent of proton transfer to the base. Protonated and unprotonated forms (**P4** and **P4H**$^+$) can be readily distinguished (Figure 6) at low temperatures, and proton exchange between them is slow on the NMR time scale below −58 °C (see the SI for full analysis of this exchange). **P4** shows two resonances, a quartet (^2J(P,P) = 15.2 Hz) at δ −17.0 and a doublet (^2J(P,P) = 15.2 Hz) at δ 11.5 in a 1:3 ratio. Protonation of **P4** results in a downfield shift of 2.7 and 7.4 ppm for the quartet (central phosphorus) and doublet, respectively. The ^2J(P,P) significantly increases from **P4** (15.2 Hz) to **P4H**$^+$ (37.4 Hz) upon protonation, consistent with increased interaction of the phosphorus atoms.

Deprotonation of carbonyl compounds with **P4** produces strongly polarized chemical shifts of the enolate species in solution compared to the enol silyl ether counter parts.[10a,b] Comparison of ^{13}C NMR shifts for **2-P4H** and **1-P4H** to **2-TMS** and **1-TMS** showed that the C—O carbon of the **P4** enolates was shifted downfield from 18 to 20 ppm while the O—C=C carbon was shifted upfield by 22 ppm. The ^{19}F NMR signals for these enolates were also significantly shifted upfield. These chemical shift changes are approximately twice as large as for the lithium enolates, a dramatic illustration of the noncoordinating nature of the phosphazenium compared to metal counterions (Table 1).

The X-ray single crystal analysis of the phosphazenium enolate **2-P4H** provided additional insights. The crystals of **2-P4H** showed two symmetry independent ion pairs with different conformations in the asymmetric unit. One enolate anion was disordered over two positions (roughly related by a 2-fold axis) in a 86:14 ratio. No direct contacts (Figure 7) were observed between the enolate and the acidic proton of **P4H**$^+$ (distance from the oxygen to the acidic hydrogen was 3.43 A), which is consistent with the strongly polarized chemical shifts of the enolate signals in solution (Table 1) and provides further evidence for the "naked" nature of **P4** enolates. Comparison of the structure of **2-P4H** with those of **2-Li**·TMTAN and (**2-Li**)$_2$ shows that the bond lengths follow the other criteria of charge delocalization, with **2-P4H** showing the shortest C—O bond, the dimer the longest, and the monomer between them. The C=C bond length follows the reverse order (Table 2).

Crystals suitable for X-ray diffraction analysis of **P4** could be obtained from a solution of commercial **P4** diluted in

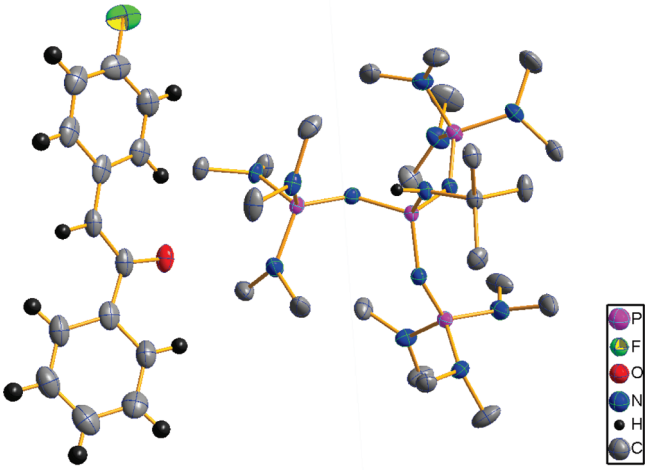

FIGURE 7. Molecular drawing with 50% probability ellipsoids of **2-P4H** determined by single crystal X-ray analysis (methyl hydrogens of **P4H**$^+$ and the minor components are omitted for clarity).

TABLE 2. Select Bond Lengths of 2-P4H, 2-Li·TMTAN and (2-Li)$_2$·THF$_4$[a]

compound	O—*C*=*C*	*O*—*C*=C	*Li*—*O*—C
2-P4H	1.3874	1.2798	
2-Li·TMTAN	1.3738	1.2937	1.7864
(**2-Li**)$_2$·(THF)$_4$	1.3588	1.3109	1.8873
			1.8733

[a]Bond lengths in angstroms; bond length error ±0.002.

THF/Et$_2$O and stored at −78 °C. This allowed a comparison of select average bond lengths of **P4** and **P4H**$^+$ (from the structure of **2-P4H**). Upon protonation the bond between the central phosphorus and the protonated nitrogen lengthens by 0.082(2) Å, while the bond lengths to the remaining nitrogen atoms shorten by an average of 0.035(2) Å (Table 3). These changes are consistent with the resonance charge delocalization **P4H**$^+$ and agree with the interpretation of NMR solution measurements.

In the course of these investigations, we also obtained a structure of **2-H**. Details are presented in the Supporting Information.

Amide Phosphazenium Enolates. Deprotonation of **3-H** with **P4** quantitatively produced **3-P4H**, with very similar NMR properties to the ketone enolates (Table 1). The *β*-enolate carbon ^{13}C NMR signal was shifted upfield by 20 ppm and the ^{19}F NMR signal by 13 ppm compared to those of the enol silyl ether.

The benzylic ketones **2-H** and **1-H** as well as a similar aldehyde enolate (*p*-fluorophenylacetaldehyde) were converted to hydrogen-bonded dimers (e.g., **2-H-2-P4H**$^+$) when 0.5 equiv of **P4** was added.[10a] Carbonyl compounds with less favorable keto−enol equilibria, such as acetophenone or methyl phenylacetate,[28] did not form stable hydrogen dimers. The behavior of **3-H** was analogues to that of these latter systems, with no detectable formation of **3-H-3-P4H**$^+$ when both **3-P4H** and **3-H** were present in solution.

(28) Guthrie, J. P.; Liu, Z. *Can. J. Chem.* **1995**, *73*, 1395–1398. Guthrie, J. P. *Can. J. Chem.-Rev. Can. Chim.* **1993**, *71*, 2123–2128. Sklenak, S.; Apeloig, Y.; Rappoport, Z. *J. Am. Chem. Soc.* **1998**, *120*, 10359–10364. Rappoport, Z.; Yamataka, H. *Chem. Commun.* **2000**, *21*, 2101–2102.

TABLE 3. Select Bond Lengths of P4 and P4H$^+$

compound		bond length (Å)
P4	*P*=*N*—*t*Bu	1.537(1)
	N—*P*=N	1.642(1), 1.645(1), 1.645(1)
	P=*N*—P	1.550(1), 1.525(1), 1.548(1)
P4H$^+$[a]	*P*—*N*—(H$^+$)*t*Bu	1.66, 1.65
	N—*P*=N	1.605, 1.629, 1.606,1.606, 1.601, 1.609
	P=*N*—P	1.574, 1.556, 1.561, 1.548, 1.544, 1.557

[a]Bond length error ±0.002.

Lithiate Species (RO)$_2$Li$^-$ (TI) and (RO)$_3$Li^{2-} (QI). Although lithium ate species (lithiates) are formed in small amounts in the presence of HMPA, much cleaner solutions were obtained by addition of P4 enolates to lithium enolates, as previously reported for **1-Li**.[10b] The **TI**[(RO)$_2$Li$^-$] is the dominant species when the ratio of P4 enolate to lithium enolate was 1:1. Past 1 equiv the higher lithiate (RO)$_3$Li^{2-} (nicknamed "quadruple ion" **1-QI**) was formed at the expense of **1-TI**. This equilibrium accurately followed eq 3. For **1-Li**, K_{eq} = 190 M^{-1}, whereas the less basic enolate of **2** showed significantly smaller K_{eq} = 4.6 M^{-1}. The dimeric and trimeric nature of **TI** and **QI** were also supported by mixed enolate experiments.[10j,12a]

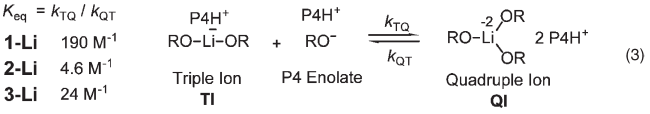

(3)

This method was applied to the lithiates generated from the amide **3-H** (Figure 8). Mixing of **3-P4H** and **3-Li** in ratios less than 1:1 produced several unidentified species, as was also observed for **2-Li** and **1-Li**. At a 1:1 ratio these were converted to a single major species, the triple ion **3-TI**, with an ^{19}F NMR signal 4.3 ppm upfield from the parent lithium dimer, and a single ^{7}Li NMR signal 0.4 ppm downfield from it. Increasing the ratio of **3-P4H** to **3-Li** to 2:1 generated a small amount of **3-QI** (K_{eq} = 24 M^{-1}, eq 3). The ^{7}Li NMR signal assigned to **3-QI**, like those of **2** and **1**, was shifted downfield by 0.95 ppm from **3-TI**, while its ^{19}F NMR resonance was shifted upfield from **3-TI** by 0.75 ppm. The

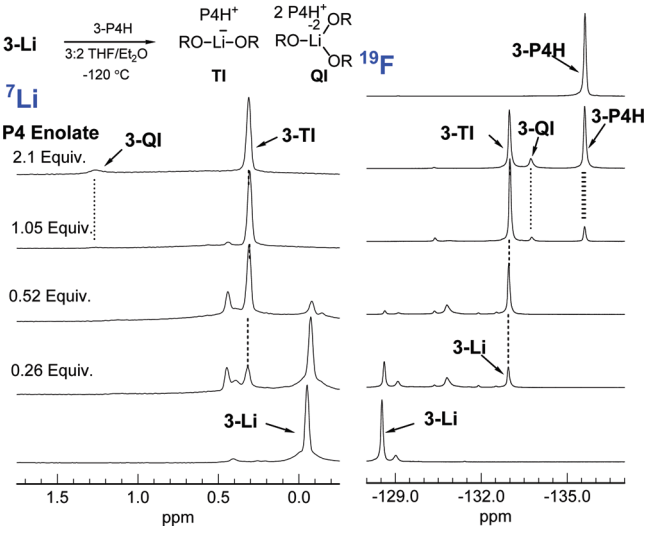

FIGURE 8. 3-P4H titration of **3-Li** to form the lithiate species (RO)$_2$Li$^-$ and (RO)$_3$Li^{2-} in THF/Et$_2$O at −120 °C.

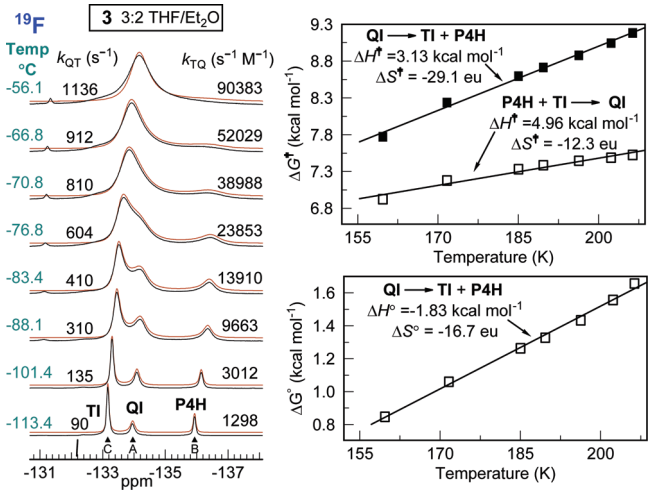

FIGURE 9. Spectra with simulated fits (red traces) of DNMR experiment of exchange of **3-TI** + **3-P4H** ⇌ **3-QI** (eq 3) in THF/Et_2O.

respective dimeric and trimeric nature of the lithiates **TI** and **QI** generated with this method was confirmed with mixed enolate experiments by using **2-Li**/**3-Li**.[16]

We had an interest in exploring the enolate reactivity of the lithiate species formed from the ketone and amide enolates. This required information about their rates of interconversion (eq 3) to establish whether the individual species could be studied under non-Curtin−Hammett conditions with RINMR.[10l,29,30] A ^{19}F DNMR study of enolates from **3-H** is presented in Figure 9. Excellent line shape fits[24] were obtained for using the three-site kinetic model of eq 3 where exchange of the **TI** and phosphazenium enolate species occurs only through formation of the **QI** species.[16] For all three enolates, the rates of interconversion are too fast for us to measure the individual reactivities of the triple ion, quadruple ion, and phosphazenium enolate under non-Curtin−Hammett conditions, which requires activation energies greater than 8.5 kcal/mol at −140 °C.[10l]

The dissociation of **3-QI** surprisingly shows a substantial negative entropy as well as entropy of activation. This suggests that the **TI** is significantly more solvated than the **QI**. The top ^7Li NMR spectrum in Figure 5 suggests that the **3-TI** is coordinated to one HMPA. Additional support for this assignment is provided by the experiment shown in Figure 10, where increments of HMPA were added to **3-TI**. A new upfield signal in the ^{19}F NMR spectrum appeared at the expense of the original **3-TI** signal. Broadening of the **TI** ^7Li resonance was also observed, possibly due to partially averaged coupling with a coordinated HMPA, but the coupling could not be resolved. Interestingly, addition of HMPA also produced NMR signals corresponding to HMPA-solvated monomers of **3-Li** (M-h_2 and M-h_3) and the P4 enolate, **3-P4H**. Apparently, not only can HMPA interact with a lithium of a triple ion species but it can also compete for lithium coordination with the enolate, causing dissociation of **3-TI** to HMPA-solvated monomers and **3-P4H**. Experiments with the lithiates of **2-H** and **1-H** showed identical behavior.[16]

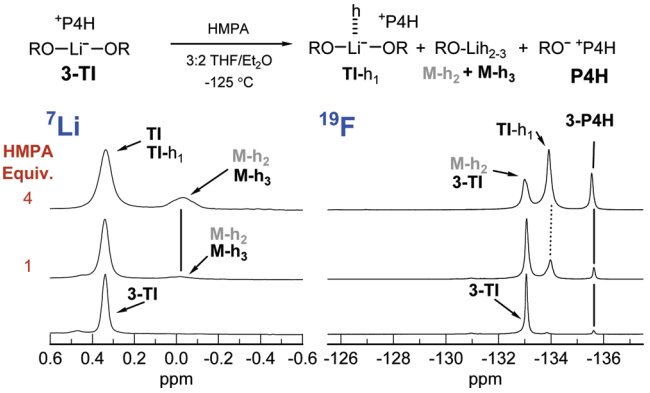

FIGURE 10. ^7Li and ^{19}F NMR spectra of HMPA titration of **3-TI** in THF/Et_2O at −120 °C (1:1 **3-Li**:**3-P4H**).

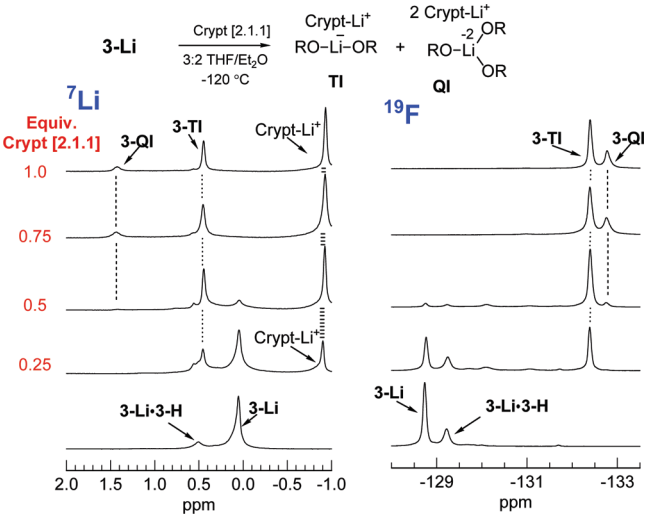

FIGURE 11. ^7Li and ^{19}F NMR spectra of Crypt [2.1.1] titration of **3-Li** in 3:2 THF/Et_2O at −120 °C.

Cryptand [2.1.1] Lithium Enolate Species. The interaction of lithium enolates with Cryptand [2.1.1] (Crypt) has been shown to form triple ions from *β*-dicarbonyl enolates.[12e,f,31] We anticipated that this lithium sequestering solvent additive would also form lithiate species from the ketone and amide enolates discussed here. Indeed titration of **3-Li** with Crypt (Figure 11) initially produced two new major ^7Li NMR signals, one upfield (−0.9 ppm), corresponding to the Crypt-solvated lithium cation, and one downfield (0.4 ppm), corresponding to the central lithium of **3-TI**. A single new ^{19}F NMR signal was also observed at a chemical shift similar to those for **3-TI** generated by using the phosphazenium/lithium enolate mixing method. The concentration of **3-TI** was maximized at 0.5 equiv of Crypt. At higher equivalents, signals corresponding to **3-QI** appear at the expense of **3-TI**.

The effect of Crypt on **1-Li** was nearly identical with the behavior observed with **3-Li**, producing both **1-TI** and **1-QI**. Examination of the interaction of **2-Li** with Crypt was hampered by solubility problems. The aggregation state of

(29) Palmer, C. A.; Ogle, C. A.; Arnett, E. M. *J. Am. Chem. Soc.* **1992**, *114*, 5619–25.
(30) Bertz, S. H.; Cope, S.; Murphy, M.; Ogle, C. A.; Taylor, B. J. *J. Am. Chem. Soc.* **2007**, *129*, 7208–7209.
(31) Cambillau, C.; Bram, G.; Corset, J.; Riche, C. *Nouv. J. Chim.* **1979**, *3*, 9. Cambillau, C.; Ourevitch, M. *J. Chem. Soc., Chem. Commun.* **1981**, 996–988. Arnett, E. M.; Maroldo, S. G.; Schriver, G. W.; Schilling, S. L.; Troughton, E. B. *J. Am. Chem. Soc.* **1985**, *107*, 2091–2099.

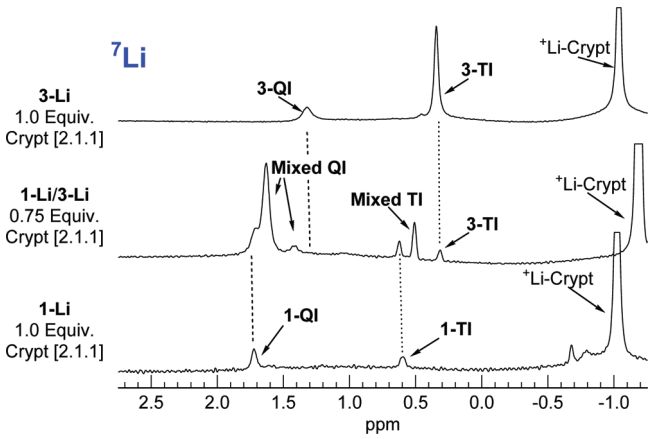

FIGURE 12. ^{7}Li NMR spectra of Cryptand [2.1.1] titration of a binary mixture of **2-Li** and **3-Li** in 3:2 THF/Et_2O.

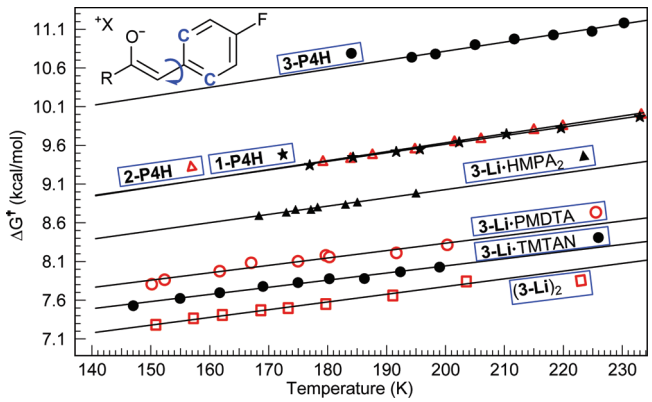

FIGURE 13. Summary of 4-fluorophenyl ring rotation of various enolate species in 3:2 THF/Et_2O as determined by ^{13}C DNMR of the *o*-aryl carbons.

the lithiates generated with Crypt was also confirmed by the mixed enolate technique (Figure 12).[16]

α-Aryl Ring Rotations. Barriers to rotation of aryl rings conjugated with carbanion centers are sensitive to the extent of charge delocalization.[10b,15b,32] The α-aryl enolates also show this effect; barriers to restricted rotation about the conjugated 4-fluorophenyl ring could be measured for a number of the enolate species by using ^{13}C DNMR methods (Figure 13). The entropy of activation for these rotations was identical ($\Delta S^{\ddagger} = -11$ to -10 eu) for the species studied. The three phosphazenium enolates **2-P4H**, **1-P4H**, and **3-P4H** show the largest barriers. The $\Delta H^{\ddagger}$ values followed the trend of the carbon acidity values of the nonfluorinated[17] carbonyl compounds (pK_a(DMSO), **2-H** = 17.7,[14a] **1-H** = 18.7,[14b] **3-H** = 26.6[14b]). Enolate **2-P4H** ($\Delta H^{\ddagger}$ = 7.33 kcal mol^{-1}) showed the lowest barrier followed closely by **1-P4H** ($\Delta H^{\ddagger}$ = 7.40 kcal mol^{-1}) and the most basic enolate **3-P4H** was significantly higher ($\Delta H^{\ddagger}$ = 8.48 kcal mol^{-1}).

For the metal bound enolates, only the enolates of **Q3-Li** showed large enough rotation barriers to be measured in THF/Et_2O. Comparison of the enthalpy of activation of the lithium dimer (**3-Li**)$_2$ ($\Delta H^{\ddagger}$ = 5.78 kcal mol^{-1}) to its phosphazenium counterpart **3-P4** showed a decrease of 2.7 kcal/mol, which clearly results from reduced charge density from the interaction with a coordinating counterion. Increased steric destabilization of the planar or near-planar ground state of the lithium versus the "naked" enolate may contribute as well. Rotation barriers in both the PMDTA and TMTAN monomers of **3-Li** were also measured. The barrier for **3-Li**·PMDTA ($\Delta H^{\ddagger}$ = 6.43 kcal mol^{-1}) was slightly higher than that of the TMTAN complex (6.20 kcal mol^{-1}) and both were higher than that of the parent lithium dimer, supporting increased charge delocalization of the lower aggregated species.

A similar DNMR experiment was performed on a solution of **3-Li** with 4 equiv of HMPA. The major species of this solution is the bis-HMPA monomer (M-h_2) but a number of species, M-h_3 and **TI**, are present as well. All species are in fast exchange in the temperature region (−105 to −78 °C) where the 4-fluorophenyl ring rotation can be measured, so the data obtained are a weighted average of these species and not exclusively the bis-HMPA monomer. The activation enthalpy for aryl ring rotation was larger ($\Delta H^{\ddagger}$ = 6.89 kcal mol^{-1}) than that of either previously studied monomers, **3-Li**·PMDTA or **3-Li**·TMTAN. This result is not surprising due to the high lithiophilicity of HMPA, which significantly decreases the interaction of the lithium with the oxygen of the enolate resulting in increased charge separation.

Conclusions

Several aggregation states, dimers, monomers, lithiates, and separated ions, of three α-aryl enolates have been investigated using multinuclear NMR and X-ray spectroscopic techniques. Through a combination of cosolvent titrations[10a,b,i] and continuous variation methods[12a] the solution aggregation states of the α-aryl enolates were determined. The ^{13}C and ^{19}F NMR chemical shifts of these enolates were found to be correlated with solution structure. The solution aggregation state identified under various conditions agreed with those observed in the solid state for enolates of **2-H**. The bond lengths of C═C observed in the X-ray crystal structures of (**2-Li**)$_2$, **2-Li**·TMTAN, and **2-P4H** were found to progressively increase, while the C—O bond length decreased in the same order. A systematic study of the barrier to rotation of the conjugated 4-fluorophenyl ring of enolate species of **3-H** found decreased aggregation of the enolate was accompanied by an increased barrier to rotation. The barrier was found to increase from aggregated contact ions, (**3-Li**)$_2$, to monomeric contact ion aggregates, **3-Li**·PMDTA or **3-Li**·TMTAN, with substantial increase observed for anions without a direct counterion interaction (**3-P4H**). The solution and solid state results are consistent with a resonance picture where lower aggregation states lead to increased delocalization of negative charge into the α-aryl ring.

Experimental Section

General. All reactions requiring a dry atmosphere were performed in glassware flame-dried or dried overnight in a 110 °C oven, sealed with septa and flushed with dry N_2. Tetrahydrofuran (THF) and Et_2O were freshly distilled from sodium

(32) Ahlbrecht, H.; Harbach, J.; Hauck, T.; Kalinowski, H.-O. *Chem. Ber.* **1992**, *125*, 1753–1762. Schade, S.; Boche, G. *J. Organomet. Chem.* **1998**, *550*, 359–379. Capriati, V.; Florio, S.; Luisi, R.; Mazzanti, A.; Musio, B. *J. Org. Chem.* **2008**, *73*, 3197–3204. Bank, S.; Dorr, R. *J. Org. Chem.* **1987**, *52*, 501–510. Yoshino, A.; Sakakihara, H.; Takahashi, K. *Bull. Chem. Soc. Jpn.* **1993**, *66*, 1323–1327.

benzophenone ketyl under N_2. Me_2O was purified by condensing several milliliters in a graduated conical flask at −78 °C from a pressurized gas cylinder, adding a small portion (0.5 mL) of *n*-BuLi, and distilling the dry Me_2O through a cannula into the desired vessel at −78 °C. *N*,*N*,*N*′,*N*″,*N*″′-Pentamethyldiethylenetriamine (PMDTA) and hexamethyl phosphoric triamide (HMPA) were distilled from CaH_2 under reduced pressure and stored over 4 Å molecular sieves under N_2. 1,4,7-Trimethyl-1,4,7-triazacyclononane (TMTAN) was purchased dry and used without further purification. Common lithium reagents and solvent additives were handled with septum and syringe-based techniques and titrated against dry *n*-propanol in THF with 1,10-phenanthroline as indicator.[33]

Low-Temperature NMR Spectroscopy. Low-temperature NMR spectra were acquired by using a 10 mm broadband probe at the following frequencies: 90.556 MHz (^{13}C), 52.984 MHz (^{6}Li), 139.905 MHz (^{7}Li), 145.785 MHz (^{31}P), and 338.827 MHz (^{19}F). All spectra were taken with the spectrometer unlocked. ^{13}C NMR spectra were referenced internally to the C−O carbon of THF (δ 67.96), Et_2O (δ 66.57), or Me_2O (δ 60.25). Lorentzian multiplication (LB) of 2−6 Hz was applied to ^{13}C spectra. ^{6}Li and ^{7}Li spectra were referenced externally to 0.3 M LiCl in MeOH (δ 0.00) or internally to $Li^{+}(HMPA)_4$ (δ −0.40). ^{31}P NMR spectra were referenced externally to 1.0 M PPh_3 in THF (δ −6.00) or internally to free HMPA (δ 26.40). ^{19}F NMR spectra were acquired without proton decoupling and were referenced internally to $CFCl_3$ (δ 0.0), 1,3-difluorobenzene (δ −110.8), or 1,2-difluorobenzene (δ −140.0). Probe temperatures were measured internally with the ^{13}C chemical shift thermometer $(Me_3Si)_3CH$.[10m]

General Preparation of Samples for Multinuclear NMR Spectroscopy. Lithium diisopropylamide (LDA) was prepared fresh before formation of an enolate solution by the following procedure. Solvent was added (typically 1.8 mL of THF and 1.2 mL of Et_2O) including 1−2 μL of ^{13}C enriched (10%) $(Me_3Si)_3CH$ as a shift thermometer[10m] to a dried thin-walled 10 mm NMR tube that had been stored under vacuum, fitted with septa, and flushed with N_2 or Ar. Silicon grease was applied to the interface between the tube and the septa before securing with parafilm for a better seal, as well as to the top of the septa to seal needle punctures. The NMR tube was cooled to −78 °C under positive N_2 or Ar pressure and diisopropylamine (42 μL, 0.30 mmol) and *n*-BuLi (120 μL, 2.5 M) were added to the solution. The solution was warmed to 0 °C in an ice bath for 5 min after which the solution was cooled to −78 °C under positive N_2 or Ar pressure. The desired carbonyl compound was then added via syringe either neat or as a solution of the carbonyl compound in the desired solvent. Samples were stored at −78 °C. The spectrometer probe was cooled to <−78 °C, the sample was inserted and the probe was shimmed on the ^{13}C FID of the THF peak. Spectra of NMR active nuclei which usually included ^{13}C, ^{31}P, ^{19}F, ^{7}Li, and ^{1}H were then acquired. At this point, a titration, variable-temperature, or variable-concentration experiment could be performed. In the case of a titration experiment, for each addition the sample was ejected and placed in a −78 °C bath, the silicon grease was removed from the top of the septum, a desired amount of cosolvent was added, silicon grease was reapplied to the top of the septum, and the desired NMR spectra were measured, including a ^{13}C NMR spectrum to determine the sample temperature.

Acknowledgment. We thank the NSF for financial support (CHE-0074657) and funding for instrumentation (NSF CHE-9709065, CHE-9304546).

Supporting Information Available: Additional spectra of all enolate experiments, cosolvent titrations, and variable temperature experiments, and X-ray crystal structure information for **P4**, *Z*-**2-P4H**, (*Z*-**2-Li**)$_2\cdot(THF)_2$, *Z*-**2-Li**·TMTAN, and **2-H**. This material is available free of charge via the Internet at http://pubs.acs.org.

(33) Watson, S. C.; Eastham, J. F. *J. Organomet. Chem.* **1967**, *9*, 165–168.